



Effect of High Flux  
X-radiation on  
Parchment

for

Abigail Quandt  
Walters Art Museum  
Baltimore, Maryland

August 27, 2005

Gregory Young  
Sr. Conservation Scientist  
Conservation Research

Report No. Proteus 92195



## Table of Contents

<b>1.0 Introduction</b> .....	2
<b>2.0 Experimental</b> .....	2
2.1 Sampling .....	2
2.2 Measurement of stability by thermal microscopy.....	3
2.2.1 Image Capture.....	3
2.3 Image Analysis and Quantification.....	4
<b>3.0 Results and Discussion</b> .....	5
<b>4.0 Conclusions</b> .....	8
<b>Appendix One: Shrinkage profiles of collagen fiber denaturation</b> .....	9
<b>Appendix Two: Statistical Analysis</b> .....	27

© *Department of Canadian Heritage*  
*Ministère du Patrimoine canadien*

*No part of this report may be reproduced or distributed in any form or by any means -  
electronic, mechanical, photocopy, or otherwise - without the prior written permission  
of the Canadian Conservation Institute of the Department of Canadian Heritage.*



---

## 1.0 Introduction

At the request of Abigail Quandt, Walters Art Museum, Baltimore, MD, a study was conducted on the physicochemical effects to parchment of exposure to high flux x-radiation. The museum is collaborating with Uwe Bergman of the Stanford Synchrotron Radiation Laboratory to employ high flux x-ray fluorescence spectroscopy to enhance the text on the Archimedes Palimpsest. The technique will map the iron in the residual iron-gall ink that is undetectable by the visible and ultraviolet illumination imaging techniques used to enhance most of the writing. By digitally mapping the residual iron, more of the writing will be revealed.

X-rays are expected to interact radiochemically with the parchment in a well-characterized manner. Absorption of x-ray photons initiates the formation of peroxy radical derivatives in proteins; this results in chain scission and cross-linking, and the evolution of volatile molecular fragments that initiate the formation of more radicals. Chain scission and alteration of amino acid side chain chemistry lead to a destabilization of protein conformation and, in the collagenous proteins of parchment, to the lowering of the stability of native structure. In this study, sensitive measurements of molecular stability were undertaken by quantitative thermal microscopy to record detectable changes resulting from exposure to x-rays at, and above, the flux levels needed to map the residual iron of the Archimedes text.

Portions of a nineteenth-century document composed of parchment were exposed to the x-radiation of the Stanford synchrotron. Microscopic surface samples of the exposed parchment were excised, immersed in water and heated in a thermal microscope from 25 °C to 80 °C at a rate of 1.0 °C/min. Digital images were captured at 0.5 °C intervals over this range. Image analysis was then employed to quantify the temperature range over which the semi-crystalline structure of the parchment samples collapsed to a gelatinous, amorphous structure by the hydrothermally induced process of denaturation. This molecular collapse of parchment manifests in the shrinkage of the sample by up to 70 %. Because of this overt response to heating, the low end of the temperature range is referred to as the shrinkage temperature ( $T_s$ ); it is to this “onset” value that the terms “thermal stability” and “stability” refer in this report. Conservation research has shown that the onset temperature drops as physicochemical deterioration advances in collagenous materials, including parchment. Exposure to x-rays was expected to lower the onset temperature of the parchment by a detectable and potentially significant amount.

## 2.0 Experimental

### 2.1 Sampling

Portions of the nineteenth century parchment were obtained from the Walters Art Museum for testing at the Stanford Synchrotron. Two tests were conducted. For “Test 1” a portion of the parchment with the word “committed”, was exposed to 6 scans for a total of  $3 \times 10^8$  photons/mm<sup>2</sup> over an region of 1 mm x 2 mm located at the rectangular area designated as “2” in

Figure 1. The photons in four of the scans had an energy of 7.9 keV and an energy of 11 keV for two of the scans. The control samples (no exposure to x-radiation) were chosen from different regions of the sample periphery, excluding location “1”. This area had been exposed during previous testing.

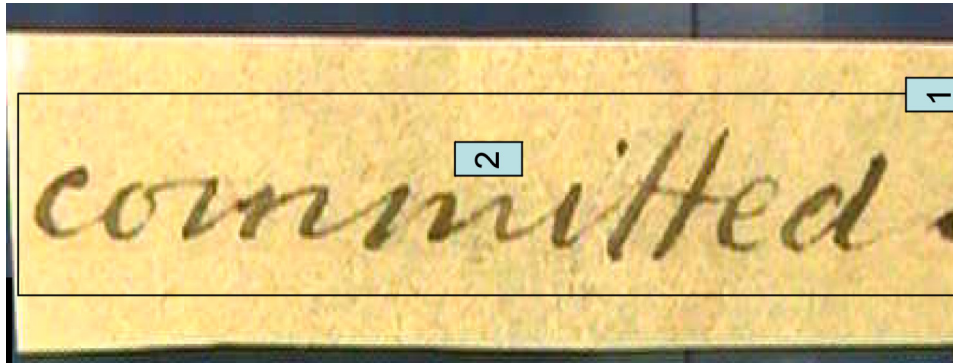


**Figure 1. Illustration of 19th C parchment fragment used in the "Test 1" measurements. The 1 mm by 2 mm region labeled "2" was exposed to x-radiation. Five samples were taken from this area for separate thermal stability measurements. Control (unexposed) sample material was taken from the periphery of the whole portion of parchment.**

Samples for “Test 2” were taken from an additional 2.5 x 1.5 cm portion of the parchment. Two separate x-ray scans were conducted. One scan exposed part of the parchment to  $5 \times 10^{11}$  photons/mm<sup>2</sup>; this was designated as “low flux” in this report. The other scan exposed the parchment to  $5 \times 10^{12}$  photons/mm<sup>2</sup>; this was designated as high flux. The energy for both scans was 8 keV.

In an attempt to differentiate the immediate and long-term effects of exposure to the synchrotron x-ray flux, accelerated aging was undertaken on the Test 2 sample material after initial thermal stability measurements were conducted. The sample was subjected to dark aging at 70 °C and 30 % RH for 2.5 months. The onset measurements were then conducted in the same manner as for Tests 1 and 2.

## **2.2 Measurement of thermal stability by thermal microscopy**

Thermal stability measurements were conducted on separate microscopic samples of the exposed and unexposed writing surface. Minute rectangular samples of the surface layer were excised and heated in water from 25 °C to 80 °C at a rate of 1.0 °C/min. using a Linkam THMA600 hot stage attached to an Olympus BX51 polarizing microscope.

### 2.2.1 Image Capture

During the temperature rise, a CoolSnap digital camera (RS Photometrics [Tucson, Arizona], 1392 X 1040 pixels, 4.65 X 4.65 µm pixel size) attached to the microscope captured an 8 bit, 256 grey scale image of the parchment fragments every 30 s, i.e. every

0.5 °C. The resulting 110 images, recorded the full temperature range and, when combined, produced a time-lapse video sequence computer file of the heat-induced denaturation (structural collapse), and thus shrinkage, of the fragments in the sample.

### 2.3 Image Analysis and Quantification

Several proprietary software programs and one public domain program were employed to undertake the quantification, including- Image Pro Plus, version 4.5.1.29, (Media Cybernetics, Inc., 1993-2003), ImageJ 1.32j (Java 1.3.1\_03; public domain) from the National Institutes of Health, USA and SigmaStat version 3.0.1 (Systat Software, Inc. 1992-2003).

The 110 gray scale images in each experiment were converted to binary images containing just black and white pixels. See **Figure 2** below. Each binary image presented a white pixel profile of the parchment sample against a black pixel background. Since images were

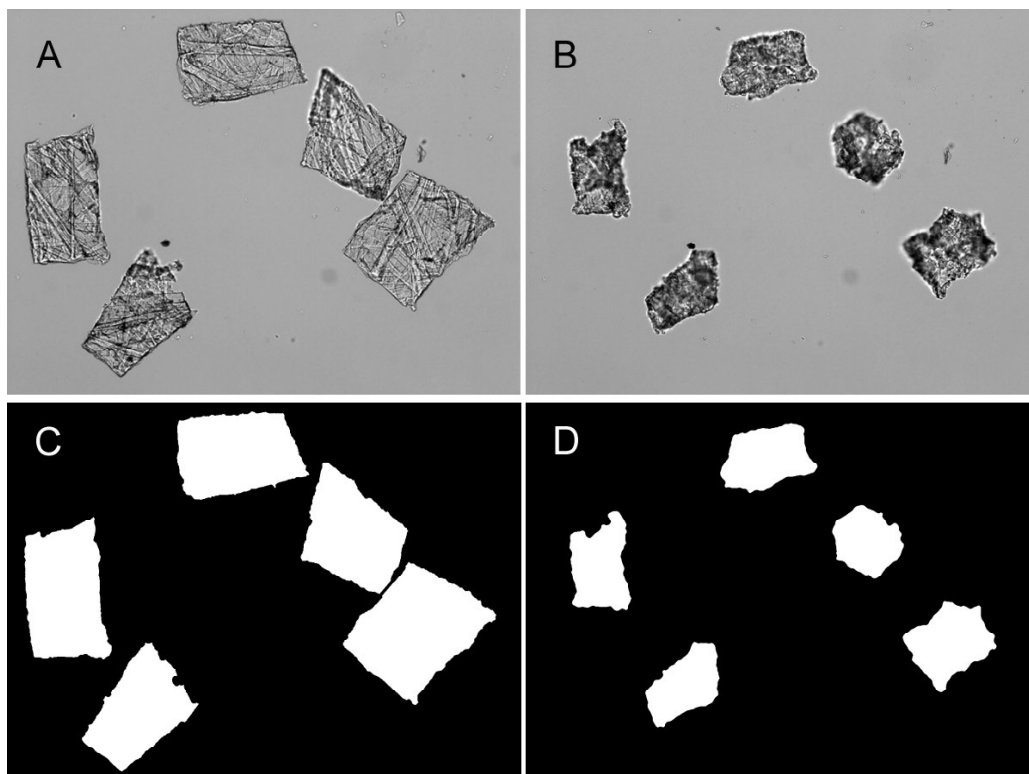
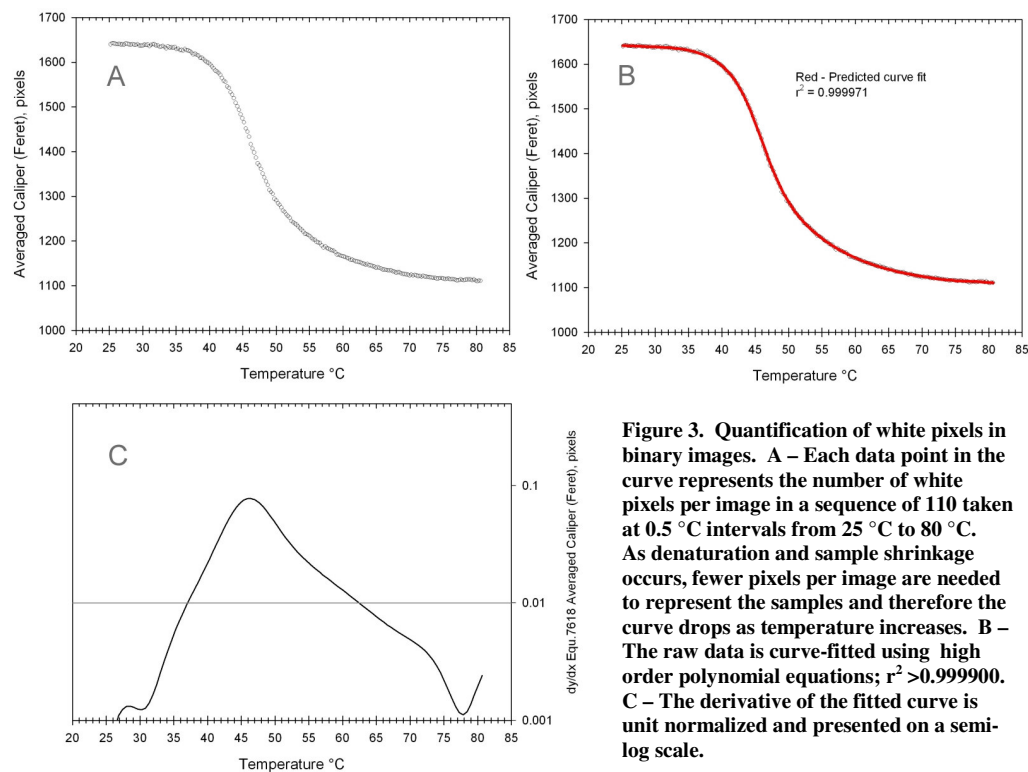


**Figure 2.** Microscopical samples cut from the surface of parchment and prepared to undergo a measurement of thermal stability. A - At the start, the samples are immersed in water at room temperature and show their full dimensions. B - At the end of a measurement, the immersed samples at 80 °C show their denatured, shrunken dimensions. C - After the experiment, the original images (e.g. A and B) were converted to binary images in which parchment samples are represented with white pixels on a black pixel background. D - Fewer white pixels are needed to represent the area of the samples after denaturation.



taken at 0.5 °C intervals over the full denaturation temperature range of the experiments, and therefore, as sample shrinkage occurred, the number of white pixels needed to represent the samples dropped in the image taken at higher temperatures. The white pixel count per image was graphed as pixels per image frame over temperature, **Figure 3a**. The best fitting high-order polynomial was chosen to smooth this raw data curve, **3b**. The unit-normalized derivative of the curve-fit was then obtained, **3c**, from which the onset temperature of the each experiment was determined. The onset temperature is the lower limit of the defined temperature range over which denaturation occurred.

### 3.0 Results and Discussion

The three graphs of **Figure 3** above were combined to produce shrinkage profiles of collagen fiber denaturation, as illustrated in **Figure 4**. The onset temperature was determined from the derivative curve at  $y = 0.01$ . The crossover of the vertical and horizontal lines in **Figure 4** marks this point on the derivative, and the vertical line crosses the x axis and the raw data (open circles) and curve-fit (red) lines at this temperature. In the example the onset is 37.0 °C. A similar profile is presented in **Appendix One** for each measurement undertaken in the study.

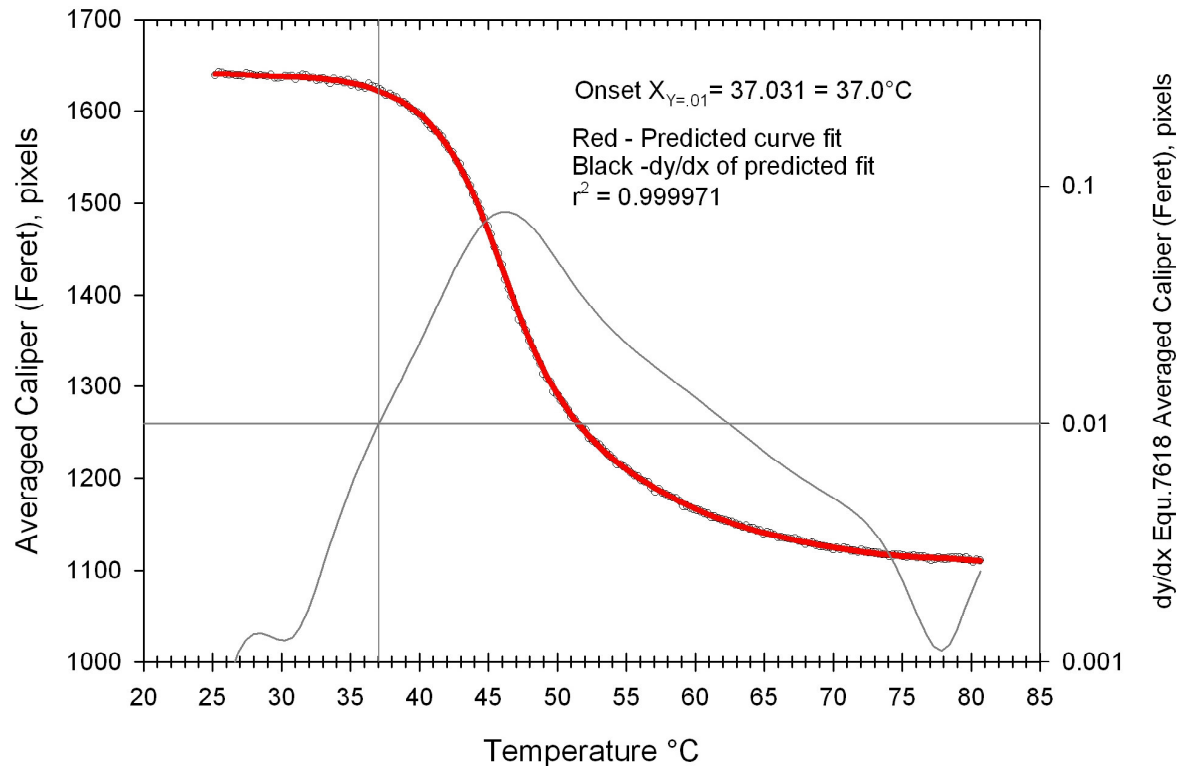


**Figure 4.** Shrinkage profile of collagen fiber denaturation. The three curves of Figure 3 were combined to produce this profile. Each experiment in this study is reported in this manner in Appendix One. The horizontal line marks the intersection of the derivative curve at  $Y=0.01$ ; the vertical line intersects this point and crosses the x axis at the corresponding onset temperature for the measurement.

**Table One:** Onset Temperatures (°C) for Tests 1 and 2 of Parchment Exposed to Synchrotron X-radiation

No.	Test 1 "Committed"	Test 1 Control	Test 2 Low Flux	Test 2 High Flux	Test 2 Control	Test 2 Low Flux Acc. Aging	Test 2 High Flux Acc. Aging	Test 2 Control Acc. Aging
1	40.43	39.56	39.92	36.53	41.79	38.60	33.40	36.40
2	37.79	38.79	36.97	38.18	40.23	35.14	33.33	34.45
3	37.61	39.32	38.25	35.11	38.71	35.68	34.55	36.66
4	38.97	40.64	41.79	37.27	43.89			
5	38.82	40.90	38.55	37.03	42.23			

**Table One** lists the onset temperatures extracted from the profiles in the appendix. The values were used to produce the box plots presented in **Figure 5**. Each box marks the 25<sup>th</sup> percentile (lower limit), median (middle horizontal line) and 75<sup>th</sup> percentile (upper limit) of the data range presented in the table for each group (column) of onset values in the table. The average of each group is reported above the box plot and is marked in the box using a dotted line.



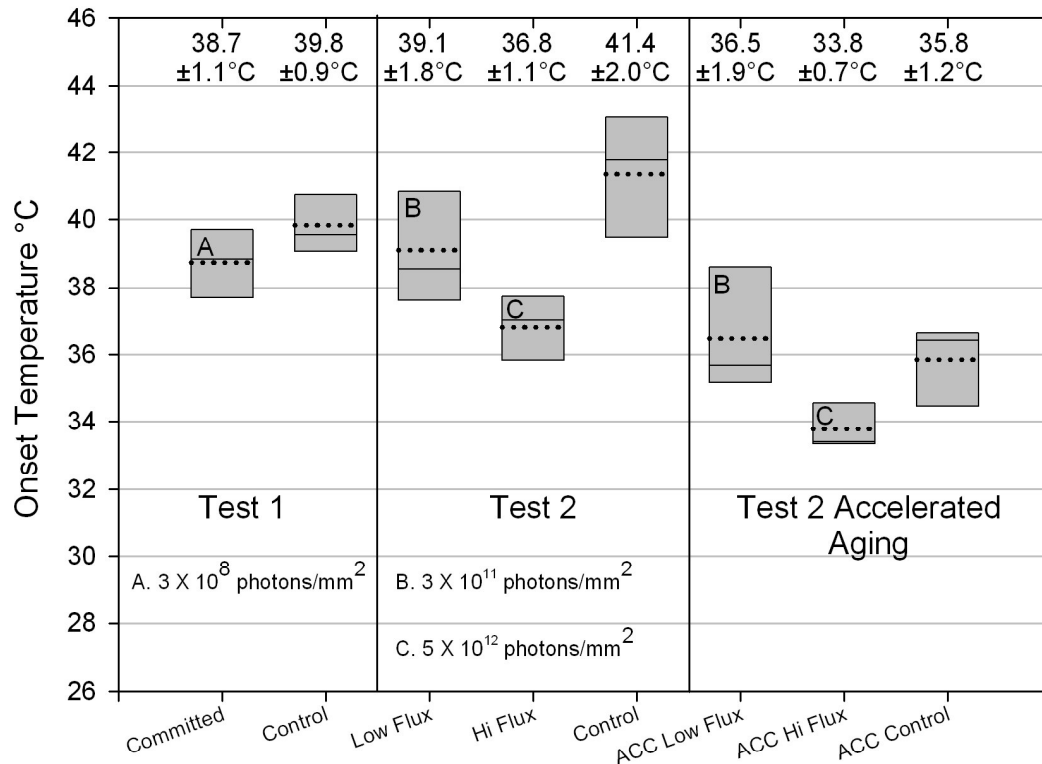


Figure 5. Box plots of onset temperatures for the eight groups of measurements conducted. The bottom and top edges of each box represent the 25th and 75th percentiles, respectively. The dotted line marks the average of the repeat measurements of each group; the values are also reported across the top. The flux exposure level is reported (A, B and C): the sample material of Test 2 was used in the accelerated aging tests and therefore had the same flux exposure.

A statistical study of the data is reported in **Appendix Two**. An analysis of variance (ANOVA) was conducted on the Test 1 and Test 2 samples, followed by a multiple pairwise comparison of the means. (It was assumed that the Test 1 and Test 2 sample material was taken from the same parchment document.) Very little difference was discovered between exposed (“Committed”) and unexposed (Control) sample portions in Test 1; just 1.1 °C separated the means. The difference was not shown to be statistically significant using the parameters employed in the current analysis (i.e., the number of repeat measurements, standard deviations of the means and the difference between the means). The results for Test 2 show a 2.1 °C drop in average thermal stability for the low flux ( $5 \times 10^{11}$  photons/mm<sup>2</sup>) exposed sample portions compared to the control and a 4.6 °C drop for the material exposed to the high flux ( $5 \times 10^{12}$  photons/mm<sup>2</sup>). The ANOVA revealed significant differences only between the mean value of the high flux and the controls for the two tests.

An ANOVA was also conducted on the Test 2 material before and after dark accelerated aging at 70 °C and 30 % RH for 2.5 months. Significant differences among the means again included the discrimination of the high flux X-ray sample portions from the Test 2 control. More importantly, the analysis showed no change in the relative stabilities of the low flux ( $5 \times 10^{11}$  photons/mm<sup>2</sup>) and the high flux exposed samples with aging.





The approximate 3 °C difference in the means between the low- and high- flux groups before aging was maintained in the sample material after aging; accelerated aging caused both groups to drop in thermal stability by approximately equal amount. Accelerated aging appeared therefore to have the same effect on the physicochemical properties of the two types of material; the high flux material was not more sensitive to accelerated aging than the material exposed to the lower flux.

Curiously, the greatest effect by accelerating aging was found with the control. The change in the mean with aging was 5.6 °C. This and the comparatively high range of values for the control before aging was unexpected and cannot be properly explained from the limited data produced in this study.

The statistical analysis suggests that, in general, exposure to high flux x-radiation did not detrimentally affect the parchment until a total exposure of approximately  $5 \times 10^{12}$  photons/mm<sup>2</sup> was attained. Below this flux, changes in thermal stability were not significantly greater than the natural variability revealed in the parchment material. Within the limits to the strength of the statistical analysis, the threshold for a significant difference between means was established in the range of 2.3 °C to 4.6 °C. The limit to the discriminating power of the analysis is, as stated above, a function of the number of repeat measurements “n”, the difference among the means and the variance of the measurements within the groups. It is possible that a greater number of repeat measurements will increase the discriminating power of the statistical analysis.

## Conclusions

Quantitative thermal microscopy was employed to measure the effects of high flux x-radiation produced at the Stanford synchrotron on the thermal stability of a nineteenth-century parchment. The results show that a 4.6 °C drop in average onset temperature from exposure to  $5 \times 10^{12}$  photons/mm<sup>2</sup> (photon energy of 8 keV) represents a statistically significant detrimental effect on the thermal stability of surface samples. No significant effect was detected for exposures to fluxes of  $3 \times 10^8$  and  $5 \times 10^{11}$  photons/mm<sup>2</sup>, based on the discriminating power of the analysis; the difference between the means of exposed and control samples was just 1.1 °C and 2.3 °C respectively. It is noteworthy that all three flux levels were consistent in causing a drop in average values of thermal stability.

Although significant statistically, the loss of thermal stability caused by the highest exposure to x-rays in this study can be considered marginal in importance with respect to the immediate effects on the parchment. The loss represents considerably less of a change than that associated with the actual manufacture of parchment. Moreover, preliminary results suggest that the long-term preservation of the parchment is not compromised. Heating at 70 °C and 30 %RH for 2.5 months had no greater detrimental effect on the samples exposed to  $5 \times 10^{12}$  photons/mm<sup>2</sup> than it did on those exposed to  $5 \times 10^{11}$  photons/mm<sup>2</sup>. The implication, although preliminary, is that exposure to the former, which produced a statistically significant effect, will have no greater influence on long-term stability than will the latter, which showed no significant effect.



Appendix Two:  
Statistical Analysis of Parchment Samples



## Descriptive Statistics: Immediate Effects and Accelerated Aging Tests after Exposure to High Flux X-radiation.

### Descriptive Statistics:

Column	Size	Missing	Mean	Std Dev	Std. Error	C.I. of Mean
Committed	5	0	38.722	1.133	0.507	1.407
Control	5	0	39.840	0.893	0.400	1.109
Test2 LoFlux	5	0	39.094	1.835	0.821	2.278
Test2 HiFlux	5	0	36.823	1.127	0.504	1.400
Test2 No X-rays	5	0	41.367	1.974	0.883	2.451
AccLoFlx 70 30	3	0	36.472	1.857	1.072	4.614
AccHiFlx 70 30	3	0	33.762	0.687	0.396	1.706
Acc Cntrl 70 30	3	0	35.836	1.206	0.696	2.996

Column	Range	Max	Min	Median	25%	75%
Committed	2.837	40.434	37.597	38.816	37.742	39.340
Control	2.103	40.891	38.788	39.558	39.190	40.700
Test2 LoFlux	4.820	41.786	36.966	38.546	37.930	40.386
Test2 HiFlux	3.063	38.177	35.114	37.031	36.172	37.495
Test2 No X-rays	5.173	43.880	38.707	41.786	39.853	42.642
AccLoFlx 70 30	3.451	38.594	35.143	35.678	35.277	37.865
AccHiFlx 70 30	1.221	34.554	33.333	33.399	33.349	34.265
Acc Cntrl 70 30	2.204	36.655	34.451	36.401	34.939	36.592

Column	Skewness	Kurtosis	K-S Dist.	K-S Prob.	Sum	Sum of Squares
Committed	0.800	0.293	0.212	0.542	193.612	7502.259
Control	0.203	-2.257	0.224	0.482	199.198	7939.161
Test2 LoFlux	0.653	0.169	0.217	0.514	195.469	7655.094
Test2 HiFlux	-0.709	1.240	0.196	0.616	184.114	6784.676
Test2 No X-rays	-0.201	-0.416	0.184	0.663	206.837	8571.900
AccLoFlx 70 30	1.572	--	0.332	0.211	109.415	3997.447
AccHiFlx 70 30	1.714	--	0.368	0.120	101.286	3420.561
Acc Cntrl 70 30	-1.646	--	0.347	0.169	107.507	3855.493



## One Way Analysis of Variance: Immediate Effects of Exposure to High Flux X-radiation

### One Way Analysis of Variance

**Data source:** Data 1 in Notebook 3 High XRay Flux on Parchment.SNB

**Normality Test:** Passed (P > 0.050)

**Equal Variance Test:** Passed (P = 0.459)

Group Name	N	Missing	Mean	Std Dev	SEM
Committed	5	0	38.722	1.133	0.507
Control	5	0	39.840	0.893	0.400
Test2 LoFlux	5	0	39.094	1.835	0.821
Test2 HiFlux	5	0	36.823	1.127	0.504
Test2 No X-rays	5	0	41.367	1.974	0.883

Source of Variation	DF	SS	MS	F	P
Between Groups	4	54.962	13.741	6.470	0.002
Residual	20	42.473	2.124		
Total	24	97.435			

The differences in the mean values among the treatment groups are greater than would be expected by chance; there is a statistically significant difference (P = 0.002).

Power of performed test with alpha = 0.050: 0.939

All Pairwise Multiple Comparison Procedures (Holm-Sidak method):  
Overall significance level = 0.05

Comparisons for factor:

Comparison	Diff of Means	t	Unadjusted P	Critical Level	Significant?
Test2 No X-r vs. Test2 HiFlux	4.545	4.931	0.000	0.005	Yes
Control vs. Test2 HiFlux	3.017	3.273	0.004	0.006	Yes
Test2 No X-rays vs. Committed	2.645	2.870	0.009	0.006	No
Test2 No X-r vs. Test2 LoFlux	2.274	2.467	0.023	0.007	No
Test2 LoFlux vs. Test2 HiFlux	2.271	2.464	0.023	0.009	No
Committed vs. Test2 HiFlux	1.900	2.061	0.053	0.010	No
Test2 No X-rays vs. Control	1.528	1.658	0.113	0.013	No
Control vs. Committed	1.117	1.212	0.240	0.017	No
Control vs. Test2 LoFlux	0.746	0.809	0.428	0.025	No
Test2 LoFlux vs. Committed	0.371	0.403	0.691	0.050	No



## One Way Analysis of Variance: Preliminary Accelerated Aging Study

### One Way Analysis of Variance

**Normality Test:** Passed (P > 0.050)

**Equal Variance Test:** Passed (P = 0.752)

Group Name	N	Missing	Mean	Std Dev	SEM
Test2 LoFlux	5	0	39.094	1.835	0.821
Test2 HiFlux	5	0	36.823	1.127	0.504
Test2 No X-rays	5	0	41.367	1.974	0.883
AccLoFlx 70 30	3	0	36.472	1.857	1.072
AccHiFlx 70 30	3	0	33.762	0.687	0.396
Acc Cntrl 70 30	3	0	35.836	1.206	0.696

Source of Variation	DF	SS	MS	F	P
Between Groups	5	142.286	28.457	11.410	<0.001
Residual	18	44.893	2.494		
Total	23	187.179			

The differences in the mean values among the treatment groups are greater than would be expected by chance; there is a statistically significant difference (P = <0.001).

Power of performed test with alpha = 0.050: 1.000

All Pairwise Multiple Comparison Procedures (Holm-Sidak method):  
Overall significance level = 0.05

Comparisons for factor:

Comparison	Diff of Means	t	Unadjusted P	Critical Level	Significant?
Test2 No X-r vs. AccHiFlx 70	7.605	6.594	0.000	0.003	Yes
Test2 No X-r vs. Acc Cntrl 70	5.532	4.796	0.000	0.004	Yes
Test2 LoFlux vs. AccHiFlx 70	5.332	4.623	0.000	0.004	Yes
Test2 No X-r vs. Test2 HiFlux	4.545	4.550	0.000	0.004	Yes
Test2 No X-r vs. AccLoFlx 70	4.896	4.245	0.000	0.005	Yes
Test2 LoFlux vs. Acc Cntrl 70	3.258	2.825	0.011	0.005	No
Test2 HiFlux vs. AccHiFlx 70	3.061	2.654	0.016	0.006	No
Test2 No X-r vs. Test2 LoFlux	2.274	2.276	0.035	0.006	No
Test2 LoFlux vs. Test2 HiFlux	2.271	2.274	0.035	0.007	No
Test2 LoFlux vs. AccLoFlx 70	2.622	2.274	0.035	0.009	No
AccLoFlx 70 vs. AccHiFlx 70	2.710	2.101	0.050	0.010	No
Acc Cntrl 70 vs. AccHiFlx 70	2.074	1.608	0.125	0.013	No
Test2 HiFlux vs. Acc Cntrl 70	0.987	0.856	0.403	0.017	No
AccLoFlx 70 vs. Acc Cntrl 70	0.636	0.493	0.628	0.025	No
Test2 HiFlux vs. AccLoFlx 70	0.351	0.304	0.764	0.050	No